# Transport of volcanic tephra layers in glaciers: a case study at Mýrdalsjökull, Iceland.

by

Alexander H. Jarosch[1], Eyjólfur Magnússon[2]

[1]ThetaFrame Solutions, Kufstein, Austria
[2]Institute of Earth Sciences, University of Iceland, Askja, Reykjavík, Iceland

RH-05-22

INSTITUTE OF EARTH SCIENCES


Jarosch, A. H.; Magnússon, E. *Transport of volcanic tephra layers in glaciers: a case study at Mýrdalsjökull, Iceland.* RH-05-22, 2022, doi:10.5281/zenodo.7108369

# Transport of volcanic tephra layers in glaciers: a case study at Mýrdalsjökull, Iceland.

Alexander H. Jarosch[1] and Eyjólfur Magnússon[2]

[1] *ThetaFrame Solutions, Kufstein, Austria*
[2] *Institute of Earth Sciences, University of Iceland, Askja, Reykjavík, Iceland*

September 23rd, 2022

## 1 Introduction

Volcanic eruptions regularly deposit extended tephra layers on glacier surfaces. Iceland with its rich and well studies volcanic history (e.g. Larsen et al., 1998) is an ideal study site for transport mechanisms within glaciers. For the work presented here, we choose the Mýrdalsjökull ice cap, with its prominent central volcano (i.e. Katla) and an extensive data availability (e.g Björnsson et al., 2000; Magnússon et al., 2021).

Our numerical simulations build on a two-component, coupled approach utilizing (I) a Full–Stokes ice-flow model and (II) a transport model. This approach allows us to simulate transport processes of initially surface deposited tephra layers in complex glacier flows, which originate from the intrinsic non-linear ice rheology (e.g. Glen, 1955) and its interplay with bed topography.

After a brief overview on the methods and data used, we present a case study of transporting a homogeneous tephra layer, initially placed just below the ice surface, for a period of 100 years with the prevailing ice flow. In this study, surface mass-balance processes and changes in ice geometry are neglected to focus on the transport mechanisms.

## 2 Methods and Data

### 2.1 Two-Component Simulation Framework

As a first step, our two-component simulation approach requires the computation of an ice flow field (i.e. ice velocity vectors for the whole simulation domain). We utilize the finite-element based Full–Stokes ice flow model Elmer/Ice (e.g. Gagliardini et al., 2013) to calculate such velocity vector fields for a given, fixed ice geometry based on field data (cf. data section 2.2 below). Finite-element methods are ideal for simulating complex geometries as found in glaciers and have proven themselves to be highly suitable for non-linear fluid rheologies as found in ice.

In a second step, the computed ice velocities are transferred to a transport model. To ensure mass/concentration conservation during the transport simulations, we apply the finite-volume based *scalarTransportFoam* solver from OpenFOAM (Greenshields, 2020). Such a transport model is often termed "passive", as it takes the velocity field in which the material (i.e. tephra layer) is transported, as input. Once the velocity field from the ice-flow model is re-projected to the computational mesh of the transport model, we can simulate the temporal evolution of a given tephra layer concentration distribution over a predefined period of time.

In our simulations at Mýrdalsjökull, the computational domain of the transport model is embedded in a larger domain for computing ice flow (cf. Fig 1). For the finite-element based ice velocity computation, we use a tetrahedral cell based mesh, whereas for the finite-volume transport computations the mesh consists of hexahedral cells. The large domain for ice flow allows us to compute physically consistent ice flow velocities for the whole ice-cap. Thus we can avoid potentially incorrect flow field results caused by boundary effects in case of limiting the ice flow domain to smaller than natural ice geometry extents.

### 2.2 Data

The bedrock DEM used for modelling is based on extensive radio echo sounding measurements. These surveys and the interpolation methods applied for the bedrock DEM are for the higher part of the Mýrdalsjökull, covering the caldera of Katla and including focus area of this modelling work is given in Magnússon et al. (2021), while the creation of the bedrock DEM outside the caldera is given in Björnsson et al. (2000). The surface DEM used on the modelling is derived from Plíades, stereo satellite images acquired in the autumn 2016 (Magnússon et al., 2021).

## 3 Results

In this study we present two simulation results to showcase the numerical capabilities of our two-component simulation framework (cf. sect. 2). The first simulation demonstrates mainly horizontal transport along an outlet glacier at Mýrdalsjökull (i.e. Kötlujökull) and the second simulation illustrates predominately vertical transport at the center of Mýrdalsjökull ice-cap.

For all simulations presented here we use a Glen flow law coefficient for temperate ice of $A = 2.6 \times 10^{-24}$ Pa$^{-3}$ s$^{-1}$ and a non-linearity exponent $n = 3$ (c.f. Cuffey and Paterson, 2010). These ice rheology parameters were inferred by matching modelled to GPS-measured ice surface velocities in low ice flow areas of Mýrdalsjökull (Jarosch et al., 2020). During the transport simulations, we set the diffusivity coefficient for tephra in ice to a numerically very small value of $D = 1 \times 10^{-9}$, as we assume no diffusion processes act on the tephra layers embedded in ice. Tephra concentrations ($\alpha_{\text{tephra}}$) within the glacier are represented on a relative volume concentration scale, i.e. as a fraction of tephra volume $V_{\text{tephra}}$ over total numerical cell volume $V_{\text{tot}}$, such that $\alpha_{\text{tephra}} = V_{\text{tephra}}/V_{\text{tot}}$.

### 3.1 Centennial scale horizontal tephra transport at Kötlujökull

We embed a large, rectangular cuboid (2500 x 2500 m) tephra deposit which reaches from the glacier surface all the way to the glacier base into the upper catchment of Kötlujökull (see Fig. 1, red box). Ice flow dynamics of this outlet glacier will transport the tephra down-glacier, through a narrow region and thereafter start to distribute the tephra within the large outlet region. Tephra is transported over a horizontal distance of approximately 14 km in the course of a 100 year long simulation.

Horizontal cell sizes for the transport model were 25 m (see Fig. 1, light blue box), whereas the larger scale ice dynamics are modelled at a horizontal cell scale of 100 m. Within the transport model sub-domain, cell sizes in the ice flow model have been refined to the same scale as the transport model.

A series of snapshots in time of the tephra transport evolution are displayed in Fig. 2. One can clearly observe the re-distribution of the initially cuboid shaped tephra distribution along the outlet glacier, with varying final tephra concentrations along the flow path. The same dataset, presented as an animation can be found at https://vimeo.com/463011819.

As can be seen in Fig. 2, the initially cuboid tephra deposit deforms during transport, following the rapid ice motion through the narrow section at Kötlujökull. Forwards the end of the simulation the tephra deposits widens again as it takes a turn following the prevailing ice flow.

### 3.2 Centennial scale vertical tephra transport at the central region of Mýrdalsjökull

For our second simulation, we embed tephra over a 6000 x 4000 m large area to a depth of 75 m below the ice surface in the central region of Mýrdalsjökull (see Fig. 1, yellow box). As tephra layers within Icelandic glaciers are normally very thin (on the order of meters), we track the bottom interface (at $\alpha_{\text{tephra}} = 0.5$) between our initial deposit and pure ice as a proxy for a realistic, thin as deposit.

At this location we have a distinct vertical flow field component, so it is an ideal location to examine vertical transport processes. Again, our simulation evolves over 100 years and a series of iso-concentration surfaces ($\alpha_{\text{tephra}} = 0.5$) are displayed in Fig. 3.

Clearly visible in Fig. 3 is a central region with strong vertical upward motion. This ice motion is a result of an ice surface depression that is present in the ice surface data and has formed in reality by geothermal heat that melts ice at the glacier bottom. Our simulation does not include this process, thus the ice flow closes this initial surface depression. After 20 years of evolution, the tephra layer in this region moved upward to the surface, whereas the

rest of the tephra layer has moved downward. Over the course of our 100 year simulation we can observe a complex tephra layer geometry forming.

### 3.3 Final remarks

Both of our simulation presented here demonstrate the potential of our numerical setup (c.f. sect. 2.1) to simulate tephra transport in complex ice flow configurations that occur in glaciers and ice-caps.

Our horizontal tephra transport simulation (cf. sect. 3.1) showcases the effectiveness of our advection scheme used in the transport model. As can be seen in Fig. 2, the lateral spreading of tephra along the flow path is dominated by advection whereas numerical diffusion has a minimal influence on the final tephra distribution after 100 years of simulation. Note that transport simulations in glaciers are notoriously hard to implement (e.g. Wirbel and Jarosch, 2020).

With our vertical tephra transport simulation (cf. sect. 3.2) we demonstrate the models' capability for tracking a thin tephra layer in a complex vertical flow field. Driven by local upward flow, tephra in the center of the domain rises to the surface, whereas the surrounding regions descend, following the prevailing flow directions. This results in an intricate, three dimensionally warped tephra layer after a 100 years of evolution.

Building upon these two model capabilities we will attempt to simulate the evolution of the 1918 tephra layer in Mýrdalsjökull as a next step. Recent data on the current tephra layer locations exists (Magnússon et al., 2021) and the here demonstrated model capabilities are vital prerequisites for such a study.

## 4 Acknowledgements

This study was financed by the Icelandic research council (Rannís) through the project Katla Kalda (nr. 163391). Pléiades imagery used to produce a DEM for 2016 was acquired at research price thanks to the CNES ISIS program. The Pléiades imagery used to produce DEMs in 2019 were provided by CNES through CEOS (Committee on Earth Observation Satellites) support to the Iceland Volcanoes Supersite.

## 5 Figures and Tables

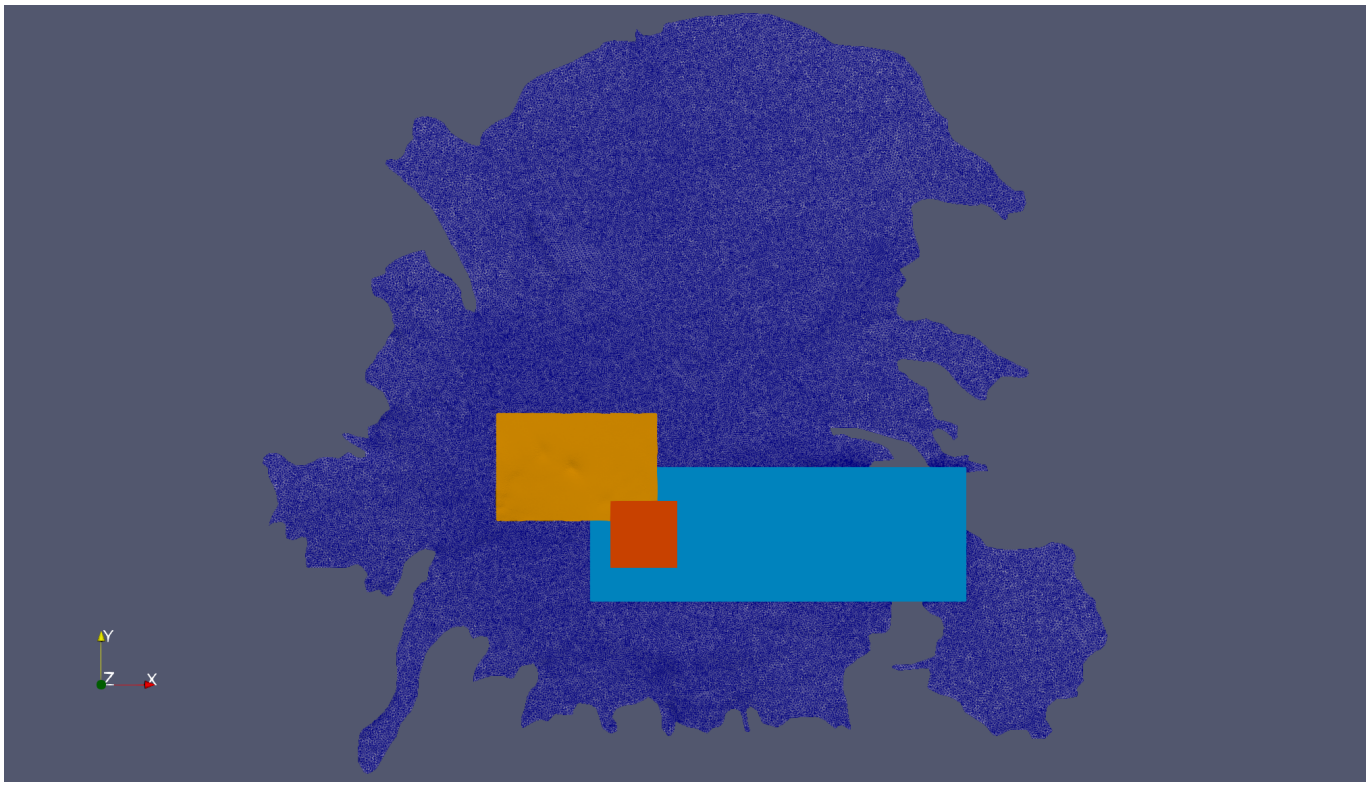


Figure 1: Computational domain for Mýrdalsjökull. The red box indicated the tephra release area for our horizontal transport experiment (cf. Sect. 3.1) and the yellow box the release area for our vertical transport experiment (cf. Sect. 3.2). Inside the light blue box (including the red box) and the yellow box we utilize a cell size of 25 m, whereas the rest of the ice-cap is simulated with 100 m cell sizes.


Initial tephra distribution at t=00.00 years.

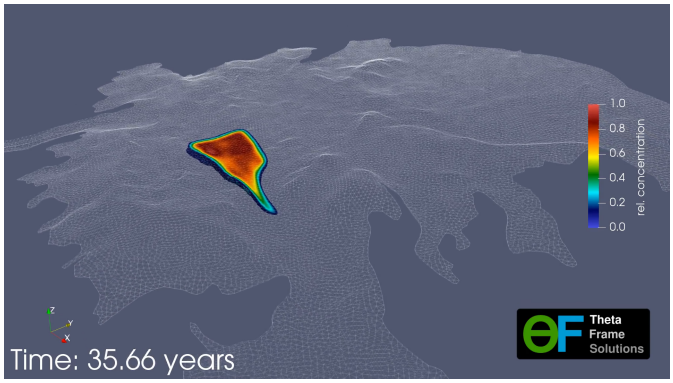


Tephra distribution at t=35.66 years.

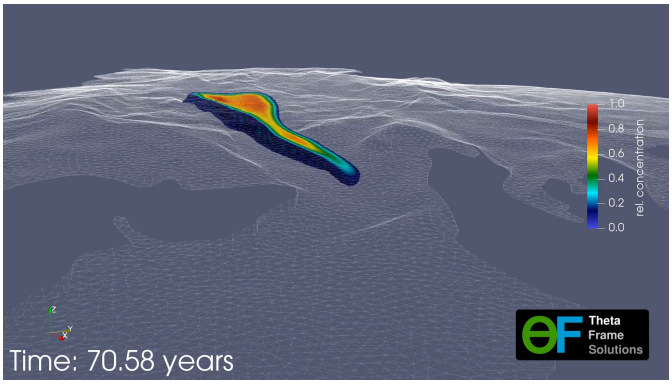


Tephra distribution at t=70.58 years.

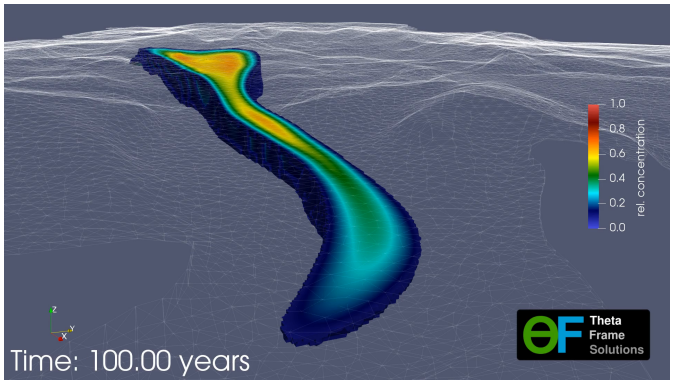


Final tephra distribution at t=100.00 years.

Figure 2: Results from the horizontal tephra transport experiment at Kötlujökull (cf. Sect. 3.1). Tephra concentrations on a relative numerical cell volume scale are displayed in colors. Mesh cells which are completely filled with tephra are displayed in bright red (rel. concentration = 1) and completely empty cells are transparent. To visualize the ice cap geometry, the tetrahedral mesh of the finite element ice velocity computation is displayed in white.

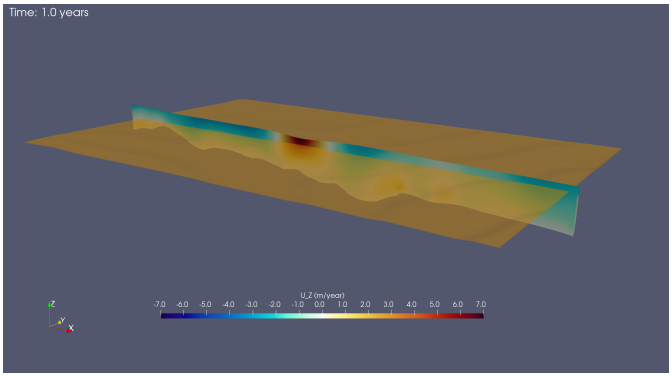


Initial tephra layer geometry at t=01.00 years.

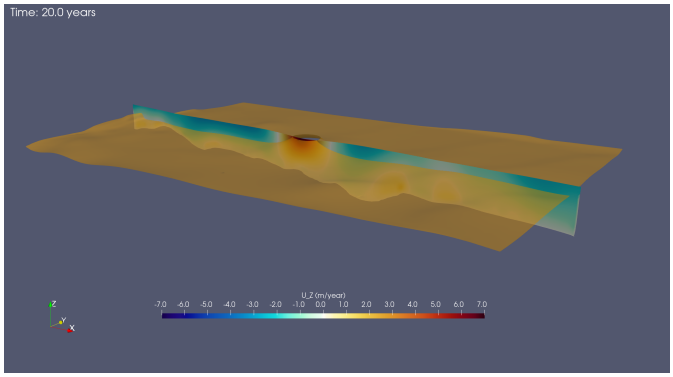


Tephra layer geometry at t=20.00 years.

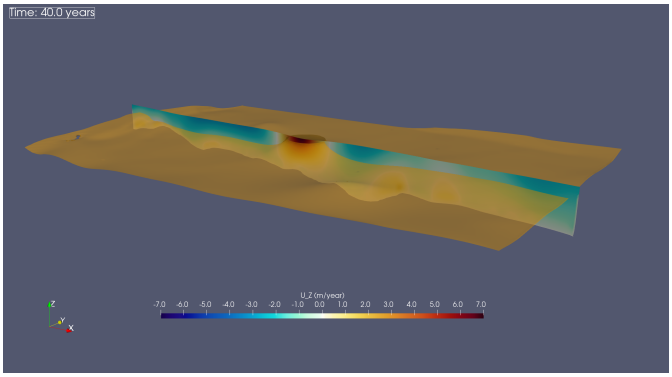


Tephra layer geometry at t=40.00 years.

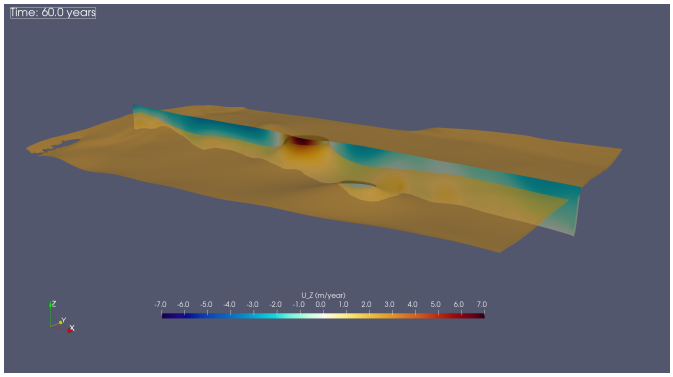


Tephra layer geometry at t=60.00 years.

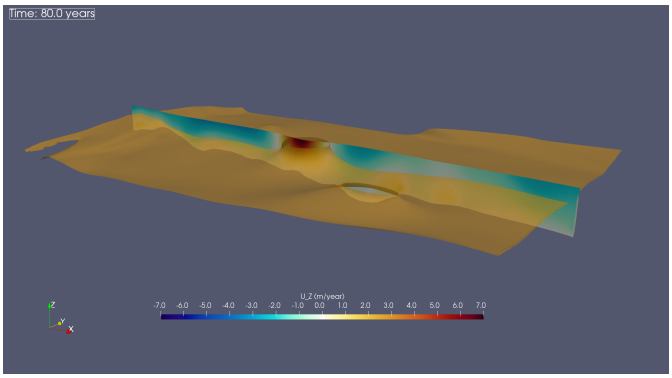


Tephra layer geometry at t=80.00 years.

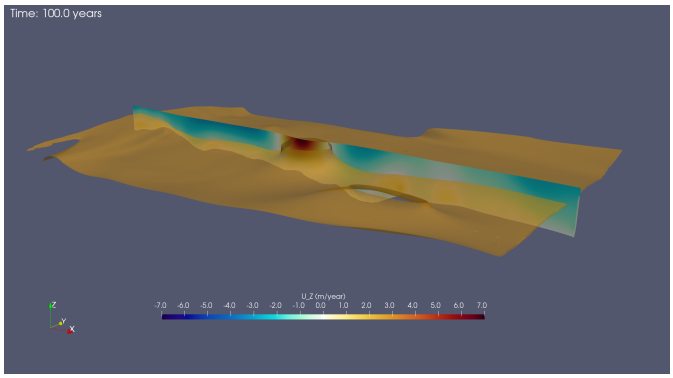


Final tephra layer geometry at t=100.00 years.

Figure 3: Evolution of a tephra layer at the center of Mýrdalsjökull (vertical tephra transport experiment, cf. Sect. 3.2). The orange, opaque surface indicates the tephra layer geometry whereas the vertical cross-section displays vertical ice velocities in m/year.

## References


Björnsson, H., Pálsson, F., and Guðmundsson, M. T.: Surface and bedrock topography of the Mýrdalsjökull ice cap, Jökull, 49, 29–46, 2000.

Cuffey, K. M. and Paterson, W. S. B.: The Physics of Glaciers, Elsevier Butterworth-Heinemann, Burlington, USA., 4th edn., 2010.

Gagliardini, O., Zwinger, T., Gillet-Chaulet, F., Durand, G., Favier, L., de Fleurian, B., Greve, R., Malinen, M., Martín, C., Råback, P., Ruokolainen, J., Sacchettini, M., Schäfer, M., Seddik, H., and Thies, J.: Capabilities and performance of Elmer/Ice, a new-generation ice sheet model, Geoscientific Model Development, 6, 1299–1318, https://doi.org/10.5194/gmd-6-1299-2013, 2013.

Glen, J. W.: The Creep of Polycrystalline Ice, Proceedings of the Royal Society A: Mathematical, Physical and Engineering Sciences, 228, 519–538, https://doi.org/10.1098/rspa.1955.0066, 1955.

Greenshields, C.: OpenFOAM v8 User Guide, The OpenFOAM Foundation, London, UK, URL https://doc.cfd.direct/openfoam/user-guide-v8, 2020.

Jarosch, A. H., Magnússon, E., Wirbel, A., Belart, J. M. C., and Pálsson, F.: The geothermal output of the Katla caldera estimated using DEM differencing and 3D iceflow modelling, https://doi.org/10.5281/ZENODO.3784657, 2020.

Larsen, G., Gudmundsson, M. T., and Björnsson, H.: Eight centuries of periodic volcanism at the center of the Iceland hotspot revealed by glacier tephrostratigraphy, Geology, 26, 943, https://doi.org/10.1130/0091-7613(1998)026<0943:ecopva>2.3.co;2, 1998.

Magnússon, E., Pálsson, F., Jarosch, A., van Boeckel, T., Hannesdóttir, H., and Belart, J. M. C.: The bedrock and tephra layer topography within the glacier filled Katla caldera, Iceland, deduced from dense RES-survey, Jökull, 71, 39–70, https://doi.org/10.33799/jokull2021.71.039, 2021.

Wirbel, A. and Jarosch, A. H.: Inequality-constrained free-surface evolution in a full Stokes ice flow model (evolve_glacier v1.1), Geoscientific Model Development, 13, 6425–6445, https://doi.org/10.5194/gmd-13-6425-2020, 2020.